AIAA 79-1724R

Digital Estimation and Control of a Seismic Isolation Platform

Gary B. Lamont* and Phillip L. Toler†
Air Force Institute of Technology, Wright-Patterson AFB, Ohio

This paper discusses the application of linear stochastic optimal estimation and control techniques for actively controlling an inertial instrument test platform. The system is modeled as a linear system with stochastic disturbances. A forced separation concept is employed in order to independently investigate the effects of a Kalman filter and an optimal controller. Optimal and suboptimal Kalman filter models are developed and evaluated at physically realizable sampling rates. A general optimal estimation and control algorithm is generated and a proposed sequence of algorithm computations presented. The results indicate that the optimal estimation and control system is capable of improving the performance of an inertial instrument test platform.

Introduction

A SEISMIC ioslation platform can be employed as an inertial instrument test platform to provide a high degree of isolation from environmental disturbances. An active control system is then needed to provide the isolation required for testing and evaluating highly advanced inertial components and systems.

As depicted in Fig. 1, an example[1] of an inertial instrument test platform is a 25×25 ft square with nine circular test tables extending approximately 2 ft from the top surface of the platform. Viewed from below, the platform is cruciform-shaped. The platform is 9 ft high, constructed of steel reinforced concrete, and weighs approximately 450,000 lb. It is supported by 20 pneumatic cylinders that essentially float it a fraction of an inch above the base slab. The pneumatic cylinders rest on red oak blocks that, in turn, rest on the base slab. The base slab rests on a compacted aggregate fill base that is designed to minimize the coupling of vibrations in order to separate the platform base from the building foundation. The inner 12 cylinders (Fig. 2) regulate the height of the platform (referenced to the base slab) and the outer 8 cylinders are used in a push-pull configuration to regulate angular motion about the horizontal axis. Azimuth motion is not controlled, only tilt motions.

The example system has a natural frequency of 1.3 Hz and effectively acts as a passive isolation system (low-pass filter) for disturbances above 1.3 Hz. Unfortunately, many of the disturbances of interest, e.g., earthquakes, ocean waves, and barometric pressure variations, have frequencies below 1.3 Hz and, therefore, an active control system is required to isolate the platform from these disturbances.

In order to provide active control of the platform, a combination of tiltmeters, angular motion sensors, and actuators are attached to the platform (Fig. 3). The eight angular motion control cylinders, in combination with the tiltmeters (on the surface of the platform), provide closed-loop control of angular motion about the platform's center of gravity. Additional damping control is provided by a second control loop consisting of angular motion sensors (seismometers) and electromagnetic one-dimensional dampers (shakers). The shakers are attached at the four corners of the platform at the approximate level of the center of gravity.

Early investigations and attempts at stabilizing the example platform were primarily analog control systems.[2-4] The analog designs, although successful in just meeting the specification for angular position, were unable to meet the angular rate requirements.

More recently, attempts have been made to provide digital control to the platform,[5] including attempts at implementing various Finite Impulse Response (FIR) and Infinite Impulse Response (IIR) filters.[6] Digital control was chosen since it is generally more flexible than analog control. Changes in sensors or actuators can often be incorporated with only software modifications. An additional benefit of digital controllers is their adaptability to the solution of stochastic optimal estimation and control problems due to accuracy requirements.

Although some design work has demonstrated the feasibility of digital control,[5,6] the actual implementations of these designs have not been successful. The failure of the implemented controllers/filters to meet the theoretical performance levels is due primarily to the effects of slow sampling rates, finite wordlengths, the uncertainties in the system models, process noise, and the sensitivities of the sensors employed.

Two investigations were completed in which the platform was modeled as a stochastic system.[7,8] Stochastic modeling of the system permitted the application of optimal estimation and stochastic control methods to the problem of test platform isolation.

Statement of the Problem

The purpose of this study was to analyze and implement an optimal estimator and controller for the active control of the seismic isolation platform. The specifications are dictated by the performance criteria for new generation inertial components.[9] These criteria require that the angular position (tilt) of the platform be maintained within ± 0.001 arc-sec and the angular rate (velocity) be maintained within $+0.001$ arc-sec/min (1.667×10^{-5} arc-sec/s). In addition, the controller must be effective in the frequency band of 0-20 Hz (Ref. 5) with a step input (for testing purposes) of 2.5 ft-lb. A step input, applied directly to the top surface of the block, is used for testing because it is easily modeled in the s domain and also in the discrete (z) domain. The 2.5 ft-lb step input was chosen because it has been demonstrated that it approximates the disturbance caused by moderate environmental disturbances on the passive platform.[8]

The system is considered to be linear over the frequency band of 0-20 Hz, and it is assumed that the construction of the platform and the locations of the sensors are such that the coupling of the modes of motion is minimized to the extent that they can be considered separately. Structural resonances above 20 Hz (the total number is unknown) are disregarded.[6]

The process and measurement noise can be modeled as white and Gaussian. The white-noise assumption is valid due to the wide-band characteristics of the system (wide-band noise driving a limited bandwidth system). The Gaussian

Presented as Paper 79-1724 at the AIAA Guidance and Control Conference, Boulder, Colo., Aug. 6-8, 1979; submitted Nov. 9, 1979; revision received Jan. 5, 1981. This paper is declared a work of the U.S. Government and therefore is in the public domain.

*Professor, Electrical Engineering Department.
†Captain, U.S. Air Force.

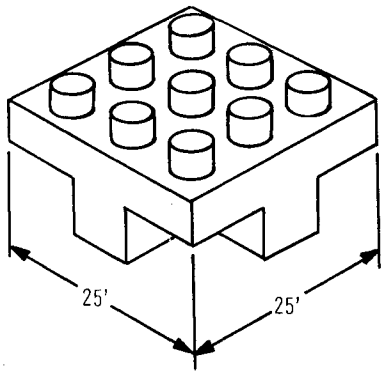

Fig. 1 Concrete block platform.

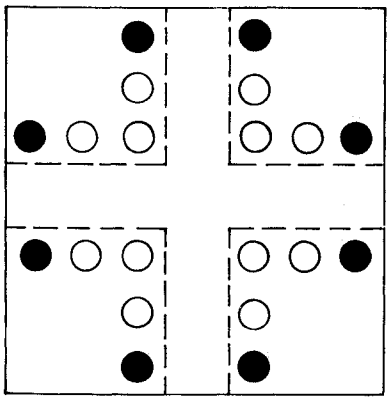

Fig. 2 Location of pneumatic cylinders: ● = angular motion control cylinders; O = height control cylinders.

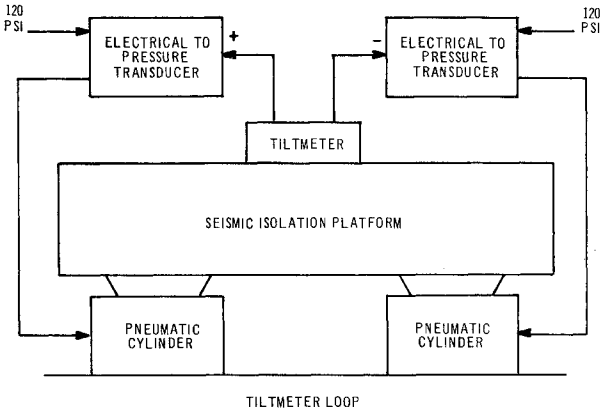

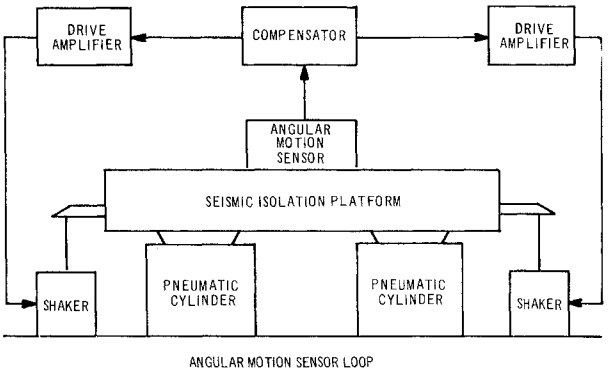

Fig. 3 Platform control loops.

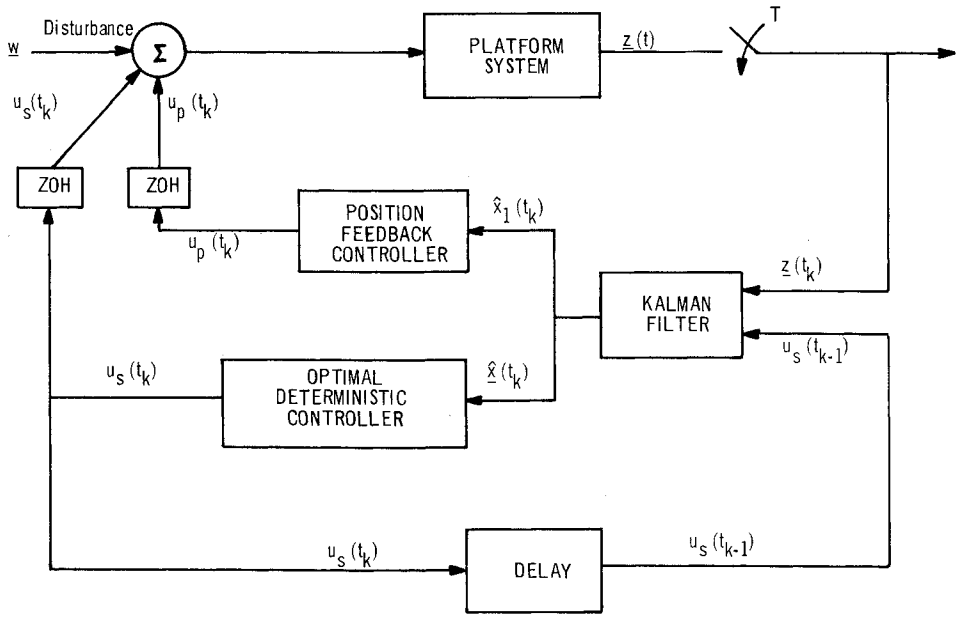

Fig. 4 Filter/controller configuration.

assumption is based on the Central Limit Theorem since the process and measurement noises are composed of several independent additive noises.[10] The process noise and measurement noise are considered to be independent.[7] This assumption is based on the fact that the sensors are separated and the measurement process does not corrupt the state being measured.

Kalman Filter Development

The development of the optimal Kalman filter is based on the state variable (truth) model of the seismic platform system composed of the platform dynamics, sensors, and process and measurement noise sources. The Kalman filter, based on this system "truth" model, i.e., the optimal Kalman filter, is used as a benchmark to determine the best performance that can be expected from the optimal estimation of the state of the seismic isolation platform system. The effects of finite wordlength, sampling rate, and noise levels are to be investigated. In addition, by making various simplifying assumptions, suboptimal Kalman filters can be developed based on reduced-order system models.

The optimal estimation problem is separated from the optimal control problem in this investigation by invoking the forced separation concept.[10] This permits the independent design and analysis of the optimal estimator (Kalman filter) without consideration of the optimal control gain. The

outputs of the Kalman filter (state estimates) become the current state inputs to the optimal controller when the controller and estimator are recombined (Fig. 4).

The platform system can be modeled as a linear stochastic system and can be represented, in state variable form, by the equation

$$\dot{x}(t) = F(t)x(t) + G(t)w(t) + L(t)u(t) \tag{1}$$

where $F(t)$ is the system matrix, $G(t)$ the matrix of states corrupted by process noise, $L(t)$ the control matrix, $x(t)$ the state vector, $w(t)$ the process noise vector, and $u(t)$ the control input vector.

The measurement equation for the system is given by

$$z(t_k) = H(t_k)x(t_k) + v(t_k) \tag{2}$$

where $z(t_k)$ is the measurement vector, $H(t_k)$ the measurement matrix, $x(t_k)$ the state vector, and $v(t_k)$ the measurement noise vector.

The matrices $F(t)$, $G(t)$, $L(t)$, and $H(t)$ are assumed to be time invariant and are therefore expressed as F, G, L, and H.

The process noise, $w(t)$, and the measurement noise, $v(t_k)$, are considered to be independent and, therefore, uncorrelated.

The process noise is described as zero-mean, white Gaussian noise. The process noise covariance matrix, $Q(t)$, is given by

$$E[w(t)w(t+\tau)] = Q\delta(\tau) \tag{3}$$

The measurement noise is described as zero-mean, white Gaussian noise and the measurement noise from the tiltmeter is assumed to be independent of the measurement noise from the seismometer. The sampled measurement noise covariance matrix, $R(t_k)$, is given by

$$E[v(t_i)v(t_k)^T] = \begin{cases} R(t_i) & (i=k) \\ 0 & (i \neq k) \end{cases} \tag{4}$$

The F, G, L, and H matrices are derived from the system transfer functions[10] (s domain).

The state variable definitions are: x_1 and x_2 are the platform phase variables (i.e., angular position and rate); x_3, x_4, and x_5 reflect the third-order tiltmeter dynamics; x_6 and x_7 represent the second-order angular motion sensor (seismometer); finally, x_8, x_9, and x_{10} refer to the states of the thrid-order noise filter for disturbance torques. The shaker dynamics are represented by a constant gain in the frequency band (0-20 Hz) of interest. The pneumatic actuator dynamics are only used in the control model (forced separation). The F matrix is

$$F = \begin{bmatrix} 0 & 1 & 0 & 0 & 0 & 0 & 0 & 0 & 0 & 0 \\ -49 & -0.7 & 0 & 0 & 0 & 0 & 0 & 2.16 & 0 & 0 \\ -3.04 & 0 & -12.6 & 1 & 0 & 0 & 0 & 0 & 0 & 0 \\ 0 & 0 & -77.6 & 0 & 1 & 0 & 0 & 0 & 0 & 0 \\ 19.84 & 0 & -198 & 0 & 0 & 0 & 0 & 0 & 0 & 0 \\ 2 & 0 & 0 & 0 & 0 & -2 & 1 & 0 & 0 & 0 \\ 1 & 0 & 0 & 0 & 0 & -1 & 0 & 0 & 0 & 0 \\ 0 & 0 & 0 & 0 & 0 & 0 & 0 & -125 & 1 & 0 \\ 0 & 0 & 0 & 0 & 0 & 0 & 0 & 0 & -125 & 1 \\ 0 & 0 & 0 & 0 & 0 & 0 & 0 & 0 & 0 & -125 \end{bmatrix} \tag{5}$$

and the G and L matrices are

$$G = \begin{bmatrix} 0 \\ 0 \\ 0 \\ 0 \\ 0 \\ 0 \\ 0 \\ 0 \\ 0 \\ 1 \end{bmatrix} \qquad L = \begin{bmatrix} 0 & 0 \\ 2.156 & 2.156 \\ 0 & 0 \\ 0 & 0 \\ 0 & 0 \\ 0 & 0 \\ 0 & 0 \\ 0 & 0 \\ 0 & 0 \\ 0 & 0 \end{bmatrix} \tag{6}$$

The control input is

$$u=\begin{bmatrix} u_p \\ u_s \end{bmatrix} \tag{7}$$

The control input u_p, associated with the pneumatic actuators, is generated by a deterministic position feedback controller that is used to directly counter any torque imbalance resulting from unsymmetrical positioning of items on the platform. The control input u_s, associated with the electromagnetic shaker activators, is generated by an optimal state feedback controller. The optimal controller is used to regulate the position feedback controller and also to control the angular rate of the platform.

The system measurement matrix H is

$$H=\begin{bmatrix} 0 & 0 & 1 & 0 & 0 & 0 & 0 & 0 & 0 & 0 \\ 1 & 0 & 0 & 0 & 0 & -1 & 0 & 0 & 0 & 0 \end{bmatrix} \tag{8}$$

A Kalman filter is a predictor-corrector type of estimator that uses a conditional probability density, conditioned on the actual measurements, to describe the probabilities of possible system states. The conditional probability density is a function of the system dynamics, initial states, and the assumed statistics of the disturbance noises. Since the conditional probability density function itself is Gaussian, it is completely described by the first- and second-order statistics, i.e., conditional mean and covariance. The general Kalman filter equations that represent these statistics are divided into two functions—those that propagate (predict) the conditional mean (optimal estimate) and the covariance, and those that update (correct) the optimal estimate and covariance at measurement sample times.

The propagation equations (in discrete form) are

$$\hat{x}(t_k^-)=\Phi(t_k,t_{k-1})\hat{x}(t_{k-1}^+)+\Gamma(t_k,t_{k-1})u(t_{k-1}) \tag{9}$$

and

$$P(t_k^-)=\Phi(t_k,t_{k-1})P(t_{k-1}^+)\Phi^T(t_k,\tau)+\int_{t_{k-1}}^{t_k}\Phi(t_k,\tau)G(\tau)Q(\tau)G^T(\tau)\Phi^T(t_k,\tau)\,d\tau \tag{10}$$

where $x(t_k^-)$ is the predited estimate vector, Φ the state transition matrix (derived from the system F matrix), and $P(t_k^-)$ the state covariance (prediction error) matrix. The superscripts "$-$" and "$+$" denote before and after a new measurement (update) is taken. The argument t_{k-1} represents the sample time of the preceding sample. The superscript T is the matrix transpose operator. Since the control input is constant between samples, the control transition matrix Γ is given by

$$\Gamma(t_k,t_{k-1})=\int_{t_{k-1}}^{t_k}\Phi(t_k,\tau)L(\tau)\,d\tau \tag{11}$$

where L is the control distribution matrix. The disturbance distribution matrix G describes which states are corrupted by process noise and the matrix $Q(t)$ is the process noise covariance matrix.

The Kalman filter update equations (in discrete form) are

$$\hat{x}(t_k^+)=\hat{x}(t_k^-)+K(t_k)[z(t_k)-H\hat{x}(t_k^-)] \tag{12}$$

$$P(t_k^+)=P(t_k^-)-K(t_k)H(t_k^-)P(t_k^-) \tag{13}$$

and

$$K(t_k)=P(t_k^-)H^T(t_k)[H(t_k)P(t_k^-)H^T(t_k)+R(t_k^-)]^{-1} \tag{14}$$

where $\hat{x}(t_k^+)$ is the updated estimate (corrected by measurement), $P(t_k^+)$ is the updated covariance (filter error) matrix, and $K(t_k)$ is the Kalman gain (optimal weighting) matrix. Variable $z(t_k)$ is the sampled measurement vector, H is the measurement matrix, and the superscript -1 above the bracketed term is the matrix inversion operator. The matrix $R(t_k)$ is the measurement noise covariance matrix where $v(t_k)$ is the measurement noise vector.

The Kalman filter model contains the state transition matrix (derived from the system F matrix), the H matrix, and the G matrix. In addition, the noise covariance matrices are required.

The covariance model of the white noise source driving the noise filter was determined using the variance of the output of the tiltmeter (angular position) with the platform in the uncontrolled mode. This mode is represented by the system dynamics platform model, the tiltmeter, and the process noise filter. The model state matrices, F_1 and G_1, are identical to F and G except for the deletion of states x_6 and x_7 (seismometer).

The rms quiescent peak-to-peak amplitude of the controlled platform is ± 0.4 arc-sec. The rms excursion, which can be considered to represent the standard deviation or 1σ value, is, therefore, 0.2 arc-sec. Since the tiltmeter has a gain of 100 mV/arc-sec, the excursion corresponds to 0.02 V output from the tiltmeter. The variance is found, by squaring the 1σ value, to be 0.0004 V.

The equivalent process noise covariance model was determined by solving for Q in the steady-state linear covariance propagation equation

$$\dot{P}(t)=0=F_1P(t)+P(t)F_1^T+G_1QG_1^T \tag{15}$$

where $P(t)$ is the time derivative of the system covariance. The diagonal elements of $P(t)$ are the variances of the states. The noise covariance matrix is a 1×1 matrix (scalar) in this model and the p_{33} element of the covariance matrix is the variance of the output of the tiltmeter (state x_3) in volts.

The process noise covariance was found by varying the value of Q until the tiltmeter variance approached the value determined for quiescent excursions. A value of 1.849×10 in. for Q resulted for the optimal Kalman model.

There have been no accurate models developed for the noise characteristics of the sensors employed in the platform control system. An estimate, however, was made by using one-half of the threshold values of the sensors as "rough" models of the 1σ noise amplitude. The noise variances are the 1σ values squared. Therefore, for the tiltmeter,[11] the threshold is 1.0×10^{-4} V and the variance is 2.5×10^{-9} V. The threshold of the seismometer is 1.66×10^{-3} V and the variance is 6.889×10^{-7} V.

Since there are two independent measurement noise sources, the measurement noise matrix R is

$$R=\begin{bmatrix} 2.5\times 10^{-9} & 0 \\ 0 & 6.889\times 10^{-7} \end{bmatrix} \tag{16}$$

Analysis of Optimal Kalman Filter Performance

Kalman filter performance can be analyzed, without actually implementing the filter, by analyzing a time history of the covariance of the estimates, P^- and P^+ (Ref. 10). This is possible because the covariance update and propagation equations, as well as the associated Kalman gain equation, are not dependent on the measurement realizations or the estimates.

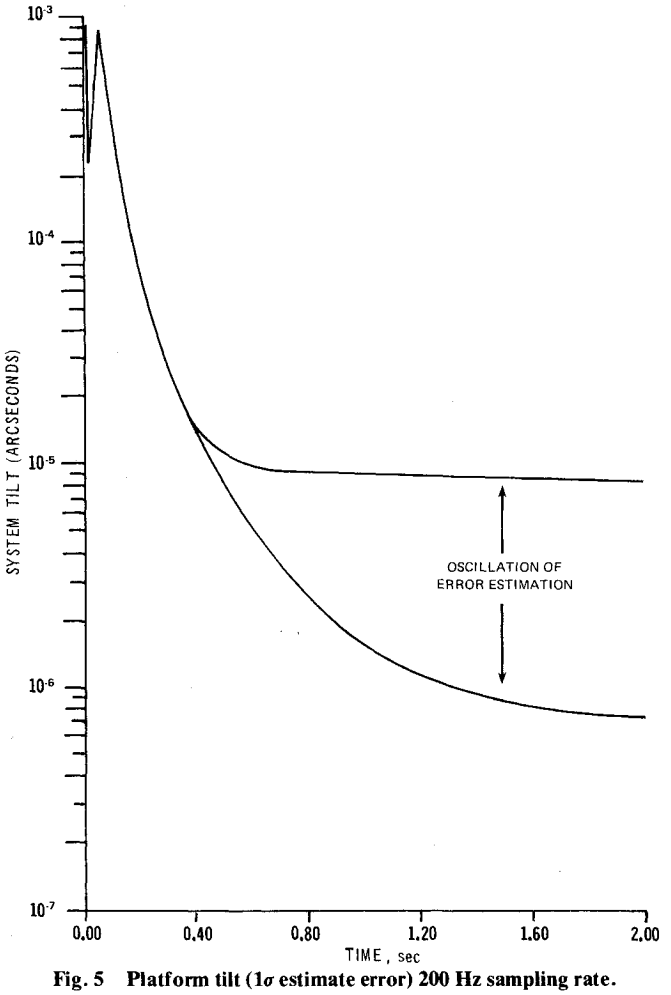

Fig. 5 Platform tilt (1σ estimate error) 200 Hz sampling rate.

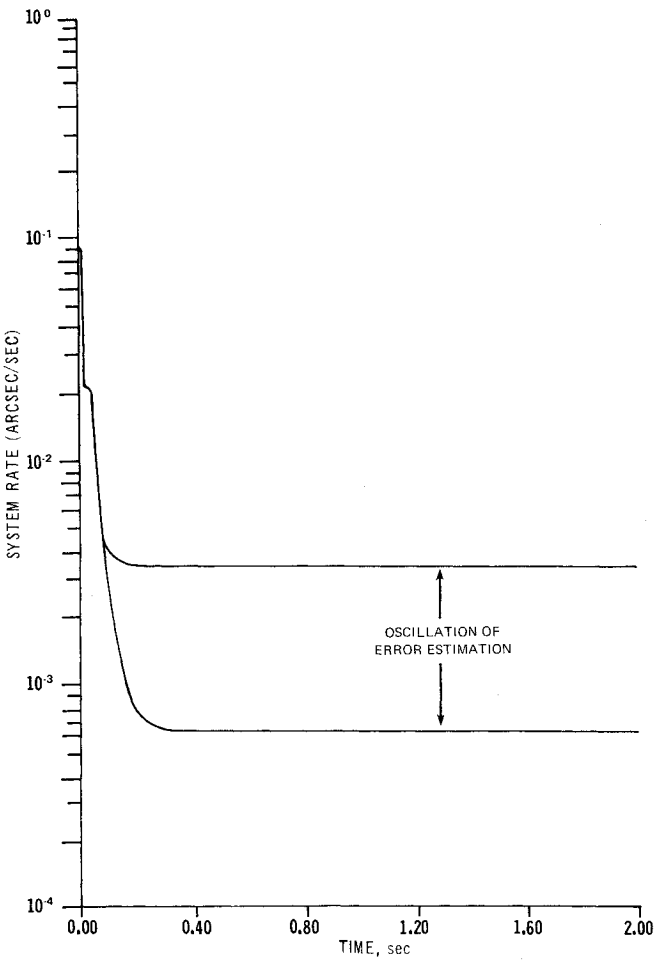

Fig. 6 Platform rate (1σ estimate error) 200 Hz sampling rate.

The time histories of the x_1 state (angular position, θ) and the x_2 state (angular rate, $\dot{\theta}$) estimate errors (1σ values), for a sampling rate of 200 Hz, are presented in Figs. 5 and 6, respectively.

The shape of the plots indicates that after an initial transient period the 1σ values for P^+ and P^- settle to steady-state conditions. This is indeed the case since it can be shown that stable time-invariant systems driven by stationary noises settle to constant 1σ values, independent of the initial state uncertainties.[12] For the seismic isolation platform, the noises are white Gaussian noise with noise strengths that do not vary with time (thus, stationary statistics) and the system matrices are time invariant. This result is important, since it permits the implementation of an approximate Kalman filter with a constant Kalman gain

$$K = P_\infty H^T R^{-1} \tag{17}$$

where P_∞ is the steady-state covariances. The Kalman filter implementation is then greatly simplified. The steady-state 1σ values are the values used for performance analysis.

Since the optimal estimates generated by the Kalman filter are used as inputs of the controllers, the design criteria for acceptable performance are that the 1σ errors in these estimates be at least as good as the required controller performance specifications, i.e., 1.0×10^{-3} arc-sec for 1σ position error and 1.667×10^{-3} arc-sec/s for 1σ rate errors. In addition, since the largest error occurs for values of P^- (just before measurement update), this error (prediction error) is used as the measurement of interest.

The 1σ prediction errors for the optimal Kalman filter, with a 200 Hz sampling rate, are $\theta = 9.05\times10^{-6}$ arc-sec and $\dot{\theta} = 3.37\times10^{-3}$ arc-sec/s. The position (tilt) prediction error (θ) is well within specifications, but the rate prediction error is more than two orders of magnitude larger than required. Since this Kalman filter is based on the "best" estimate of the physical system, the results indicate that a Kalman filter will not provide the required accuracy with a 200 Hz sampling rate!

One postulated improvement is to sample at a higher rate since, as the sampling interval becomes shorter, the prediction error decreases. To test this postulate, time histories were generated at various sampling rates from the Nyquist frequency (40 Hz) to 200 kHz. The 1σ prediction errors obtained from this analysis are presented in Table 1.

With a three-order-of-magnitude increase in the sampling rate (from 200 Hz to 200 kHz), only slightly more than a one-order-of-magnitude decrease in the angular rate error occurs. Obviously, a 200 kHz sampling is impossible to implement and, in fact, a sampling rate that high would invalidate the white noise assumptions. However, by analyzing the filter at extreme sampling rates, some insight is gained about performance bounds of the filter. Of course, the large sampling rate sensitivity is due primarily to the seismometer bandwidth of only 1 rad/s. Therefore, it is concluded that it is not possible to meet the rate prediction error criteria with the platform, actuators, and sensors as presently configured at any physically realizable sampling rate!

Since it might be possible to improve the prediction error by decreasing the error (noise) sources, an analysis of the effects of decreasing the process noise or increasing the sensitivities of the sensors was performed. The results of that analysis (in the form of 1σ prediction errors) are presented in Table 2. This prefiltering of the measurement noise may relieve the Kalman filter of high sampling rate requirements.

Table 1 Comparison of 1σ prediction errors at different sampling rates

Samping rate	Angular pos error, arc-sec	Angular rate error, arc-sec/s
40 Hz	5.7×10^{-4}	4.5×10^{-2}
50 Hz	3.1×10^{-4}	3.3×10^{-2}
100 Hz	4.4×10^{-5}	9.9×10^{-2}
200 Hz	9.05×10^{-6}	3.37×10^{-3}
2 kHz	6.7×10^{-7}	2.4×10^{-4}
200 kHz	1.4×10^{-7}	9.0×10^{-5}

Table 2 Effects of decreasing the error sources

Case	Type of improvement	1σ tilt error, arc-sec	1σ rate error, arc-sec/s
1	No change	9.05×10^{-3}	3.37×10^{-3}
2	One-order-of-magnitude reduction of process noise	4.9×10^{-6}	1.6×10^{-3}
3	One-order-of-magnitude increase in seismometer sensitivity	6.5×10^{-6}	2.8×10^{-3}
4	One-order-of-magnitude increase in tiltmeter sensitivity	8.4×10^{-6}	3.1×10^{-3}
5	Both case 3 and case 4	4.1×10^{-6}	1.9×10^{-3}

As expected, the prediction error is most sensitive to changes in the noise associated with the angular acceleration measurement (the seismometer sensitivity), but a one-order-of-magnitude increase in sensitivity (reduction in measurement noise) does not significantly reduce the prediction error. Even with the sensitivities of both sensors improved by one order of magnitude, the prediction error is far above the specification. It is concluded, then, that improvements in the sensors in the present configuration, will not significantly bring down the filter rate prediction error.

The error is due primarily to the fact that the rate estimate is based on a position measurement and an acceleration measurement. With a direct measurement of the angular rate, it is possible that the Kalman filter would provide estimates for the rate that are accurate within the specified levels.

Since it has been concluded that the optimal Kalman filter will not meet the performance criteria with the system as presently configured, and since this study is constrained to the analysis of the system as it presently exists, two approaches for further analysis were considered. The first approach is to neglect the angular rate specification and design the simplest Kalman filter that will meet the angular position specification. The second approach is to design the Kalman filter that meets or exceeds the angular position specification and, in addition, provides the smallest angular rate prediction error. It is the latter approach that was taken.

The analysis completed to this point has not considered the effects that accrue from the implementation of the Kalman filter on a small, relatively slow computer. The filter performance will be degraded further due to the limitations of the smaller machine. These degradations are discussed as part of the algorithm design and implementation considerations.[11]

As noted previously, the Kalman filters in this investigation can be modeled as constant Kalman gain filters. This is a result of the fact that the covariances (both propagated and updated) reach steady-state values, for all of the system states, after an initial transient period. The transient period is short, compared to the time the platform is in use. Thus, after an initial "warm-up" time for the filter (equal to the transient time for the covariances to reach steady state), a constant Kalman gain filter can be used. The constant Kalman gain implementation greatly reduces the computation time required by the filter algorithm because the covariance equations and the Kalman gain equation, which are the most time-consuming computations in the filter algorithm, are not computed as a part of the real-time filter. A constant Kalman gain implementation also eliminates the often severe numeric difficulties caused by the covariance update equation that normally drives the wordlength requirements. The numeric difficulties often drive the implementation of the Kalman filter to some type of square-root form, e.g., *U-D* factorization, to overcome the large wordlength requirements.[12] Since the covariance update equation does not drive the wordlength consideration in this investigation, an eigenvalue test was used to determine wordlength requirements.

In order to determine what wordlength is required to implement the optimal Kalman filter, the effects of quantization on the system eigenvalues were examined. The wordlength is acceptable only if a 10% criterion[7] is met by each eigenvalue. The wordlength, where all the eigenvalue shifts are less than 10%, is 13 bits. The fact that a 16-bit minicomputer has more bits than required allows more flexibility in scaling and lessens the effects of overflow due to arithmetic operations.

Reduced-Order Kalman Filter

Since the optimal Kalman filter is based on a ten-state model, the number of computations required to implement the filter limits the range of possible sampling rates. Thus, it is possible that a reduced-order model (suboptimal Kalman filter) might provide a smaller prediction error, since a higher sampling rate could be employed.

In order to investigate this possibility, four suboptimal Kalman filter models were developed.[11]

The noise filter provides a sharp cutoff for frequencies above approximately 20 Hz. Since the 20 Hz bandwidth of the noise from the process noise filter (exponentially correlated) is much greater than the 1.3 Hz natural frequency of the platform, the noise is assumed to be white (limited bandwidth system driven by relatively broadband noise). This simplifying assumption results in a reduced (approximate) model composed of seven states. Since, as indicated by the frequency response, the process noise filter attenuated the process noise by approximately 125 dB, a rough estimate of the equivalent white noise for the reduced model is

$$Q_{eq} \simeq 10^{-13} Q_{Ts} = 1.849\times10^{-1} \tag{18}$$

where Q_{eq} is the estimated equivalent white noise strength and Q_{Ts} is the process noise covariance used in the truth model for the system.

In order to reduce the tiltmeter model, a second-order approximation was developed that has approximately the same frequency response as the tiltmeter truth model (third order).[7]

The frequency response of the reduced-order model has the same general shape as the true model. The responses are identical at very low frequencies (up to approximately 2.5 Hz), and differ by at most 1 dB (beyond 20 Hz). However, the reduced-order model will inject additional inaccuracies (noise) into the system.

The seismometer exhibits essentially no dynamics in the 0-20 Hz frequency band and is approximated by a constant gain of one. This simplifying assumption reduces the system by two states. Two reduced models were developed using this approximation. First, in order to investigate the effects of the seismometer reduction in combination with the true tiltmeter model, a five-state model was developed. The five-state model consists of the platform dynamics model (two states), the true tiltmeter model (three states), the reduced-order siesmometer model (constant gain of 1), and the reduced-order noise filter model (constant strength white noise). Second, in order to

investigate the effects of the combination of the reduced-order models, a four-state model was developed. The four-state model consists of the platform dynamics (two states), the reduced-order tiltmeter model (two states), the reduced-order seismometer model (constant gain of 1), and the reduced-order noise filter model (constant strength white noise). Using various sampling rates, a general covariance analysis program was employed to determine the expected performance bound for each Kalman filter model.

A seven-state suboptimal Kalman filter model was also developed based on a simplifying assumption which approximated the third-order noise filter model with a roughly equivalent white noise model. The Kalman filter tuning process consists of inserting pseudonoise into the reduced-order model, by increasing the strengths of the process noise (matrix Q) and/or the measurement noises (matrix R) until the true system error approximates the error generated by the reduced-order filter. The steady-state prediction errors are 3.34×10^{-4} arc-sec for angular position and 3.78×10^{-2} arc-sec/s for angular rate. The steady-state optimal filter prediction errors are 2.53×10^{-4} arc-sec for angular position and 2.92×10^{-2} arc-sec/s for angular rate.

In the process of tuning the six-, five-, and four-state suboptimal Kalman filters, the preliminary results indicated that the error performances from those filters were far worse (on the order of 200 arc-sec/s for the 1σ rate prediction error) than the performance indicated for the higher-order filters.

The performance evaluation indicated that, based on the maximum permissible sampling rates, the optimal Kalman filter provides better performance than any of the suboptimal filters. However, the performance of the seven-state filter should not be eliminated from implementation consideration since the errors are of the same magnitude as those of the optimal filter.

Controller Development

The development of the controller segment is based on discrete models of the platform and the actuators (pneumatic cylinders and shakers). The design of the controller segment was divided into two tasks. Each control task is associated with one of the two types of actuators used in controlling the angular motion about the horizontal axis. The justification for the separation of the controller segment is based primarily on the dynamic characteristics of the actuators. The pneumatic actuators are slow (time constant of 20 s) and are actually part of the platform support system. Due to the pneumatic actuators' dynamic response, they are employed in a position feedback loop to counter any torque imbalances resulting from unsymmetrical loading of the platform. The shakers have a faster dynamic response and are employed in an optimal state-feedback control (optimal regulator) loop to regulate the effects of the environmental disturbances. In both cases, the control loops were developed with the assumption that they are receiving perfect information about the system states from the Kalman filter.

The optimal regulator is designed to regulate the pneumatic loop. The states associated with the pneumatic actuator are the contents of registers in the computer (derived from the pneumatic loop compensator algorithm) and are known exactly. These states are incorporated into the optimal control algorithm through the use of an augmented state space model that is used in deriving the control law. Assuming the exact values of the states (from the Kalman filter and from the pneumatic loop), the deterministic discrete-time optimal controller will minimize the discrete performance index.[13]

Two discrete models were derived from the continuous system transfer functions. A z-domain function, $\theta(z)$, of angular position of the platform, with a step input, was derived for use in designing the controller for the pneumatic control loop. A discrete state representation of the platform and the actuators was developed for use in the designing of the optimal controller in the regulator loop.

The pneumatic loop includes, along with the platform $G_b(s)$, and the pneumatic actuator, $H_p(s)$, an impulse sampler, a computer algorithm, $D(z)$, and a digital-to-analog converter, DAC. The impulse sampler in the model represents the estimation process completed by the Kalman filter [denoted $\theta^*(s)$]. The DAC is represented by a zero-order hold (ZOH), $H_0(s)$. $H_0(s)$ holds the output of the DAC constant between samples.

The computer algorithm, $D(z)$, is an executing digital computer program (digital controller or compensator) that receives the estimated angular position from the Kalman filter and produces a control signal $C_D^*(s)$, that is, in turn, sent to the DAC and converted to analog form for input to the pneumatic actuator.

The location of the computer in the feedback loop prohibits the reduction of the block diagram to the z-domain transfer function $\theta(z)/u_t(z)$. Instead, the approach is to solve for an expression of $\theta(z)$. Then

$$\theta(z)=\frac{u_tG_b(z)}{1+G_bH_pH_0(z)D(z)} \tag{19}$$

The z-transforms $u_tG_b(z)$ and $G_bH_pH_0(z)$ must now be determined. Since the design objective is to meet the specified response characteristics for a step input, $G_b(s)$ is evaluated with

$$u_t(s)=1/s \tag{20}$$

and

$$\mathcal{Z}[u_t(s)G_b(s)]=\frac{Bz^2+Cz}{(z-1)(z^2+\beta z+\epsilon)} \tag{21}$$

where

$$\alpha=Ae^{-aT}\sin(bT-\emptyset)$$
$$\beta=-2e^{-aT}\cos(bT)$$
$$\epsilon=e^{-2aT}$$
$$B=k_b(\beta-\alpha+1)$$
$$C=k_b(\alpha+\epsilon)$$

The z-transform for $G_b(s)H_p(s)H_0(s)$, since $H_0(s)$ is a zero-order hold, is

$$G_bH_pH_0(z)=\frac{z-1}{z}\mathcal{Z}\left[\frac{G_b(s)H_p(s)}{s}\right] \tag{22}$$

Now

$$\mathcal{Z}\left[\frac{G_b(s)H_p(s)}{s}\right]=\frac{Jz^4+Lz^3+Mz^2+Nz}{(z-1)(z-\delta)(z^2+\beta z+\epsilon)} \tag{23}$$

where

$$J=G+k-E$$
$$L=\beta k_b-\beta E+e-\delta k_b+H-\delta G-G$$
$$M=\epsilon k_b-\epsilon E+\delta\beta k_b+E\beta+\delta G-H\delta+H$$
$$N=\delta\epsilon k_b+\epsilon E+\delta G$$

To verify the discrete models, an initial value verification was employed. For verification, the initial values of the continuous time functions were compared to the initial values for the corresponding discrete-time functions.[10]

Since the zero-order hold device maintains the control inputs constant over the sampling period, the continuous state space model is transformed to a discrete state space model by the following transformation:

$$\Phi=e^{FT} \tag{24}$$

The continuous state equation is

$$\dot{x}(t) = Fx(t) + Lu(t) \tag{25}$$

with $u(t)$ for $t\epsilon[kT,\ (k+1)T]$, and the discrete state equation is

$$x(k+1) = \Phi x(k) + \Gamma u(k) \tag{26}$$

Using phase variable form state equations to represent the individual transfer functions, the resulting state matrices are

$$F = \begin{bmatrix} 0 & 1 & 0 & 0 & 0 \\ -49 & -0.7 & 1 & 1{,}725{,}430 & 0 \\ 0 & 0 & -0.05 & 0 & 0 \\ 0 & 0 & 0 & 0 & 1 \\ 0 & 0 & 0 & -24{,}649 & -219.8 \end{bmatrix} \tag{27}$$

and

$$L = \begin{bmatrix} 0 & 0 & 0 \\ 0 & 0 & 0 \\ 0.05 & 0 & 0 \\ 0 & 0 & 0 \\ 0 & 1 & 0 \end{bmatrix} \tag{28}$$

where

$$\theta = 2.156\, x_1(t) \qquad \dot{\theta} = 2.156\, x_2(t) \tag{29}$$

and

$$u(t) = \begin{bmatrix} u_p(t) \\ u_s(t) \\ u_t(t) \end{bmatrix} \tag{30}$$

The criteria used in designing the pneumatic loop compensator $D(z)$, are that the system remains stable with $D(z)$ in the feedback loop, that $D(z)$ drives the platform to zero steady-state angular position, and that the transient response (peak overshoot and settling time), to a 1.25 ft-lb input, of the controller platform meet specifications. The designed form for the discrete controller for the pneumatic loop was

$$D(z) = \frac{7500(z-0.99900)(z^2-2.0150z+1.0158)}{(z-1.0)(z^2-0.9752)} \tag{31}$$

The response of the system, with the compensator, was determined by evaluating the difference equation (transformed form $\theta(z)$ with the above $D(z)$ in the feedback loop).[6] The steady-state response for the controlled system is zero (vs 0.055 arc-sec for the uncontrolled platform), and the peak overshoot is slightly less than that for the uncontrolled platform (0.097 arc-sec vs 0.102 arc-sec). However, the settling time is slightly greater for the compensated system (approximately 11 s vs 10.86 s). The $D(z)$ described above was designed based on a sampling rate of 200 Hz. It is assumed, for analysis purposes, that the general form of $D(z)$ is maintained through the change in sampling rate. This assumption is based on the fact that changes in the sampling rate will cause changes in the locations of the roots of the discrete system models (platform and pneumatic actuator), but will not change the order of these models.

The regulator (shaker) loop is used to provide further damping of the pneumatic lop and also to provide control of the angular rate of the platform. The shaker receives its control input from a state feedback control law (optimal controller) that is based on an augmented system state model consisting of the discrete state space model of the inertial instrument test platform and actuators combined with a discrete model of the pneumatic compensator.

The state space model of $D(z)$ is[11]

$$x_D(k+1) = \begin{bmatrix} 0 & 0 & 0 \\ -0.999 & 1.0 & 0 \\ -0.999 & 0 & 0.975 \end{bmatrix} x_D(k) + \begin{bmatrix} 1 \\ 1 \\ 1 \end{bmatrix} \theta(k) \tag{32}$$

$$C_D(k) = 7500\{[-0.999 \quad 3.36324\times10^{-2} \quad -7.36435\times10^{-2}] \times x_D(k) + \theta(k)\} \tag{33}$$

Thus, the design of the control law, $C(t_k)$, is assumed independent of the stochastic properties of the system.

The quadratic performance index can be interpreted as a "system error plus control effort" measure of performance that uses a tradeoff between system error, represented by quadratic term involving the V matrix, and control effort, represented by the quadratic control "intensity" term involving the U matrix.[14]

The procedure used to solve for $C(t_k)$ consists of solving the equations

$$C(t_k) = \{U + \Gamma_P^T[V + P(k+1)]\}\Gamma^{-1T}[V + P(k-1)]\Phi \tag{34}$$

and

$$P(k) = \Phi^T[V + P(k+1)][\Phi - \Gamma C(k)] \tag{35}$$

backward in time from the terminal condition

$$P(n) = V_f \tag{36}$$

It has been demonstrated that the solution results in a steady-state solution for $C(t_k)$ that is independent of the terminal condition. The resulting control law is time invariant and asymptotically stable.[8]

The solution of the optimal control law does not guarantee that the design specifications will be met. The optimal control law must be solved by the iterative process of selecting various values for the weighting matrices, V, V_f, and U, and evaluating the resulting control law to determine if it meets the design specifications.

Results indicate that, for the control law based on a sampling rate of 200 Hz, the angular rate specification is not met, although the system does settle to within the design specification (1.667×10^{-5} arc-sec/s) within 0.08 s. It was concluded that the angular rate specification could not be met, at any physically realizable sampling rate, by the design optimal controller, due to the fact that the angular rate of the inertial test platform was already three orders of magnitude greater than the design specification at the end of the first sample period (0.05 s). The optimal controller controlled the angular position to less than 2.9×10^{-4} arc-sec, and the angular velocity to less than 2.24×10^{-2} arc-sec/s, and settled to $\pm1.6\times10^{-5}$ arc-sec/s within 0.08 s.

Conclusions

As presently configured, the platform tilt angular rate uncertainty specification cannot be met at any physically realizable sampling rate. The failure to meet this specification is due primarily to the fact that there is no direct measurement of platform angular rate.

The platform tilt angular position specification can be met by the optimal Kalman filter with a sampling rate of 45 Hz. In addition, the angular position control specification can be met based on a sampling rate of 200 Hz and the assumption that the Kalman filter provides estimations that are accurate within the angular position specification.

Acknowledgments

The authors wish to acknowledge the use of the Air Force Frank J. Seiler Research Laboratory facilities as well as the many helpful conversations with laboratory personnel, especially Bill Simmons.

References

[1] Wittry, J.P., "Description of an Inertial Test Facility Incorporating a Passively Isolated and Actively Stabilized Platform," AIAA Paper 69-863, AIAA Guidance, Control, and Flight Dynamics Conference, Princeton, N.J., Aug. 1969.

[2] Lorenzini, D.A., "Active Control of a Pneumatic Isolation System," AIAA Paper 72-843, AIAA Guidance and Control Conference, Stanford, Calif., Aug. 1972.

[3] Wynne, M.W., "A Classical Analysis into the Stability and Control of the F.J. Seiler Seismic Isolation System," Software Sciences Corp., TR74-110, Colorado Springs, Colo., March 1973.

[4] Broderson, E., "Stabilization of a Seismic Isolation Block for Inertial Instrument Testing," AIAA Paper 74-857, AIAA Mechanics and Control of Flight Conference, Anaheim, Calif., Aug. 1974.

[5] Lamont, G.B., "Digital Control of a Pneumatic Isolation System for Inertial Testing," AIAA Paper 73-830, AIAA Guidance and Control Conference, Key Biscayne, Fla., Aug. 1973.

[6] Grimes, G., FJSRL Report Contract #F05611-76-90203, Kappa Systems, Inc., Colorado Springs, Colo., Aug. 1978.

[7] Brunson, R.L., "An Optimal State Estimator for the FJSRL Instrument Test Platform," Air Force Institute of Technology, Wright-Patterson AFB, Ohio, March 1976.

[8] Burkhart, M.J., "A Digital Controller for Horizontal Angular Motion of the FJSRL Seismic Isolation Platform," Air Force Institute of Technology, Wright-Patterson AFB, Ohio, June 1976.

[9] Lorrain, P., "Low Natural Frequency Vibration Isolator or Seismograph," *Review of Scientific Instruments*, Vol. 45, No. 2, Feb. 1974, pp. 198-202.

[10] Toler, P.L., "Analysis and Implementation of Optimal Estimation and Control for the FJSRL Seismic Isolation Platform," MS Thesis, Air Force Institute of Technology, Wright-Patterson AFB, Ohio, Dec. 1978.

[11] Simmons, B.J., "Multi-Sensor Measurement of the Motion Stability of an Active Controller Isolation Test Pad," AIAA Paper 75-181, AIAA Guidance and Control Conference, Boston, Mass., Aug. 1975.

[12] Maybeck, P.S., *Stochastic Models, Estimation, and Control*, Vol. 1, Academic Press, New York, 1979.

[13] Kwakernaak, H. and Sivan, R., *Linear Optimal Control Systems*, John Wiley and Sons, Inc., New York, 1972.